

# Resveratrol-loaded $\beta$ -Lactoglobulin Nanofibrils to Prevent Enzymatic Browning on Sliced Apple

Praveetha Senthilkumar<sup>1</sup>, Vladimir Shavrov<sup>2</sup>, Petr Lega<sup>2</sup>, Ramesh Subramani<sup>\*1</sup>

1-Department of Food Processing Technology and Management, PSGR Krishnammal College for Women, Coimbatore, Tamilnadu, India.

2-TheKotel'nikov Institute of Radio Engineering and Electronics, Russian Academy of Sciences, Moscow, 125009, Russia.

## Abstract

**Background and Objective:** Resveratrol is a polyphenol with nutraceutical health benefits used as anticancer, antioxidant and anti-inflammatory with cardio protective effects. However, resveratrol lacks solubility and bioavailability and is affected by UV light, which decrease its use in food industries. It is possible to overcome these problems by loading resveratrol with appropriate biomaterials. Beta-lactoglobulin is known to form well-defined nanofibrils with various uses. The objective of this study was to use  $\beta$ -lg nanoscaled fibrils to increase bioavailability of resveratrol as well as preserving freshness and preventing enzymatic browning of sliced apples.

**Material and Methods:** Novel composite nanofibrils were prepared by loading resveratrol on Beta-lactoglobulin nanofibrils using simple self-assembly method. Furthermore, atomic force microscopy, scanning electron microscopy, *in-vitro* release assay, weight loss, total acidity, total phenolic content and antioxidant activity studies were carried out to verify the biochemical sustainable release and bioavailability.

**Results and Conclusion:** Atomic force microscopy and scanning electron microscopy images showed the formation of well-defined composite nanofibrils with an average aspect ratio of 1000; as shown in other studies. *In-vitro* release assay revealed that resveratrol was successfully loaded on nanofibrils due to possible hydrogen bonding interactions and other non-covalent linkages. The highest encapsulation efficiency of 61.1% was achieved using low concentrations of resveratrol (10mg in 1ml), whereas encapsulation efficiency of 48.3% was achieved for high concentrations of resveratrol (20mg in 1ml). The assessed weight loss, total acidity, color, total phenolic content and antioxidant activities showed ~50% increases in the shelf-life and prevention of enzymatic browning due to improved bioavailability of resveratrol. The current study could successfully demonstrate antioxidant potency of resveratrol in sliced apples and help better protections against ageing. The formula can be used as a protective layer on high-value food products such as fruits susceptible to deteriorative conditions.

**Conflict of interest:** The authors declare no conflict of interest.

## How to cite this article

Senthilkumar P, Shavrov V, Lega P, Subramani R. Resveratrol-loaded  $\beta$ -Lactoglobulin Nanofibrils to Prevent Enzymatic Browning on Sliced Apple. *Appl Food Biotechnol.* 2022; 9 (1): 9-16. <http://dx.doi.org/10.22037/afb.v9i1.35674>

## Article Information

### Article history:

- Received 2 Aug 2021  
- Revised 26 Aug 2021  
- Accepted 25 Oct 2021

### Keywords:

- $\beta$ -lactoglobulin
- Nanofibrils
- Resveratrol
- Self-assembly

### \*Corresponding author:

**Ramesh Subramani \***  
Department of Food Processing Technology and Management, PSGR Krishnammal College for Women, Coimbatore, Tamilnadu, India.

Tel: +91 6380232402

E-mail: [ramesh.subramani@psgrkwc.ac.in](mailto:ramesh.subramani@psgrkwc.ac.in)

## 1. Introduction

In recent decades, several methods have been developed to prepare nanofibrils. Examples of these methods include electro spinning, phase separation, template synthesis and self-assembly. In past few years, preparation of the nanofibrils was carried out using electro-spinning due to continuous fabrication of the fibrils and its versatility [1].

However, this method represents few problems, including low yield, fibril deposition in various substrates and high operating voltage [2]. Self-assembly offers fast, simple and low-cost strategies that produce high-ordered and stable nanostructures [3]. Non-covalent interactions are the key like hydrogen bonding, electrostatic interactions,  $\pi$ - $\pi$  interactions



and hydrophobic bindings that drive the self-assembly process. Compared to synthetic biopolymers, natural biopolymers have been established as potential candidates for the development of functionalized nanofibrils due to their uniformity, specificity, biocompatibility and crystallinity. Of the common biopolymers, whey protein is an interesting choice because of its functional group, abundance in nature and high essential amino acid content, which can be used as a gelling, emulsifying and binding agent in foods [4]. Composition of the whey protein includes bovine serum albumin of nearly 10%,  $\alpha$ -lactalbumin ( $\alpha$ -lac) of 15-20% and  $\beta$ -lactoglobulin ( $\beta$ -lg) of nearly 50% [5]. The  $\beta$ -lg includes molecular weight of 18 kDa, one  $\alpha$ -helix, eight anti-parallel  $\beta$ -chains and 162 amino acid residues [6], which has extensively been used in foods. The  $\beta$ -lg exists as a monomer at low ionic strength and pH, leading to the formation of highly-stable nanofibrils [7].

Resveratrol is a plant synthesized polyphenol (trans-3,4,5 trihydroxy-stilbene) [8], it is biologically active and used as an anti-cancer, anti-oxidant, anti-inflammatory and cardio protective agent. Mulberries, grape skins, jack fruits and peanuts are the major sources of resveratrol. It helps to decrease adverse effects of free radicals on food products during storage. Resveratrol in red wines decreases risks of coronary heart diseases, called as French paradox [9]. Lin et al. showed that resveratrol could be used as an ingredient of the cosmetic formulations for facial skin drug delivery [9]. Resveratrol is used to protect the outer tissues of fruits and vegetables due to its high antioxidant activity [10]. Therefore, resveratrol plays key roles in various applications, including increases in bioavailability of the food products. Several strategies are available to increase the bioavailability; however, use of nanofibrils as scaffolds can be effective due to their extended surfaces. In addition, preparation of resveratrol-loaded nanofibrils decreases UV-light interference to increase its photo stability and solubility. For example, resveratrol was loaded in zein fibrils, which improved the bioavailability using electro-spinning method [11]. Chitosan/poly-D,L-lactic-co-glycolic acid (CS/PLGA) microcapsules were prepared to encapsulate resveratrol and showed controlled releases and long-term protections [12]. The aim of this study was to use  $\beta$ -lg nanoscaled fibrils (less than 10 nm in diameter) as scaffold materials to attach to resveratrol and increase the bioavailability, which can preserve enzymatic browning and preserve freshness of sliced apples.

## 2. Materials and Methods

### 2.1. Materials

In general,  $\beta$ -lactoglobulin (L3908), resveratrol (R5010), 2,2-diphenyl-1-picrylhydrazyl (DPPH) (D9132) and Folin-Cio calteu reagent (F9252) were purchased from Sigma-Aldrich, USA. Hydrochloric acid was provided by Isochem

Laboratories, India. Dialysis membrane (LA395) was purchased from Himedia Laboratories, India. Red apples were purchased from a local market, Coimbatore, India.

### 2.2. Preparation of $\beta$ -lg nanofibrils and resveratrol-loaded $\beta$ -lg nanofibrils

The  $\beta$ -lg powder (2% w w<sup>-1</sup>) was dissolved in double distilled water (DW) and pH adjusted to 2 using 0.1N HCl. The resulting solution was centrifuged for 30 min at 1165×g and the residues were discarded to remove undissolved materials. The  $\beta$ -lg solution was heated at 80 °C for 10 h with constant agitation (1000 rpm) using Eppendorf Thermo Mixer C-F 1.5, Germany. This solution was used as control for further characterization. To prepare resveratrol loaded  $\beta$ -lg nanofibrils, resveratrol was dissolved in double DW (2% w w<sup>-1</sup>) and the resulting solution was centrifuged for 30 min and residues were discarded to remove undissolved materials. Then, prepared  $\beta$ -lg solution was added to the prepared resveratrol solution and heated at 80°C for 10 h with constant agitation at 1000 rpm. The resulting solution (resveratrol-loaded  $\beta$ -lg nanofibrils solution) was used for further characterization.

### 2.3. Atomic force microscopy of nanofibrils

Surface topography of the self-assembled nanofibrils was studied using AFM (atomic force microscopy) (NTM-DT, NTEGRA, Russia). Samples were diluted 100 times and 10 $\mu$ l of the fibril solutions were transferred evenly onto newly cleaved surface of mica sheets. Samples were air dried for the observation of surface topography. Analysis was carried out using contact mode at room temperature.

### 2.4. Scanning electron microscopy of nanofibrils

Morphology of the self-assembled nanofibrils were studied using SEM (scanning electron microscopy) (Zeiss Model Evo18, USA). Samples were diluted 100 times and 10  $\mu$ l of the fibril solutions were transferred evenly onto newly cleaved surface of mica sheets. Samples were air dried for the observation of surface topography. Sample was sputter coated using gold thin layers. Fibrils were analyzed using SEM microscopy of 15000× magnification.

### 2.5. Fourier-transform infrared spectroscopy of nanofibrils

Fourier-transform infrared spectroscopy (FT-IR) was carried out on  $\beta$ -lg nanofibrils, resveratrol solution and resveratrol-loaded  $\beta$ -lg nanofibrils to verify interactions between resveratrol and  $\beta$ -lg nanofibrils using Shimadzu IR Spectroscopy, Japan. The FT-IR was recorded in the wavelength range of 400-4000 cm<sup>-1</sup>. To ensure that only loaded resveratrol was attached not the unbounded resveratrol, the resveratrol-loaded solution was filtered using 0.5- $\mu$ m millipore member filters and washed three times to remove the free resveratrol. The precipitate was resuspended and used for further analysis.



## 2.6. Edible coating of nanofibrils on sliced apples

Apples were rinsed delicately and parched the sides using tissue papers and then were peeled and sliced into consistent shapes and sizes. After slicing the apples, they were weighed and coated with resveratrol-loaded  $\beta$ -lg nanofibrils and transferred into Petridishes. Dipping was carried out directly by immersing the sliced apples for 30 s and rotating them for 360° to ensure uniformity of the coating. Then, these were exposed to the atmospheric condition. Samples without coating were used as controls and the coated and uncoated samples were exposed to atmospheric condition and the following analysis were carried out for 7 h with 1-h time intervals.

### 2.6.1. Acidity

Total acidity of the coated and uncoated apples were analyzed by grinding the apples to prepare juices using blender. Briefly, 6 g of the juices were weighed and added to 50ml of DW and titrated against 0.1 N NaOH. The formula for calculating total acidity was as follows [13]:

Total acidity (%) = [(NaOH used (ml)  $\times$  0.1 N  $\times$  milli equivalent factor) / grams of the sample]  $\times$  100

### 2.6.2. Weight loss measurement

Physical weight loss (expressed as moisture loss) of the sliced apples was studied. Weight differences of the coated and uncoated samples were studied with 1-h time intervals. Weight loss was calculated using the following formula [11]:

Weight loss (%) = [(initial weight of fruit – weight of the fruit at a particular time) / initial weight of the fruit]  $\times$  100

### 2.6.3. Color analysis

Surface colour of the control (pH 2 acidic solution),  $\beta$ -lg nanofibrils, resveratrol solution and resveratrol-loaded  $\beta$ -lg nanofibrils coated apple slices were measured using Lovibond Tintometer, UK. The whiteness index (WI), chroma (C) and total color difference ( $\Delta E$ ) were calculated using the color space values (L, a and b) and the Eq.1 & 2:

$$WI = 100 - (\sqrt{(100 - L)^2 + (a)^2 + (b)^2}) \quad \text{Eq.1}$$

$$C = \sqrt{((a)^2 + (b)^2)}$$

$$\Delta E = \sqrt{((L - L_c)^2 + (a - a_c)^2 + (b - b_c)^2)} \quad \text{Eq. 2}$$

where  $L_c$ ,  $a_c$  and  $b_c$  were the color values of the control.

### 2.6.4. Total phenolic content

Briefly, 20  $\mu$ l of the extract and 1 ml of Folin-Cio calteu reagent were mixed together and then 1 ml of 10%  $\text{Na}_2\text{CO}_3$  was added to this mixture and a volume of 5 ml was made using ethanol. Solution was stored in dark for 2 h and absorbance was measured at 765 nm using UV-visible spectroscopy.

### 2.6.5. Antioxidant activity

Antioxidant activity of the coated and uncoated apples was analyzed using 2,2-diphenyl-1-picrylhydrazyl (DPPH) scavenging method [11]. Briefly, 3mg/25 ml of DPPH solution were prepared using methanol. Then, 1 ml of the DPPH solution incubated at room temperature for 30 min (at various concentrations of 50-250 $\mu$ l) was stored in dark and its absorbance was measured at 517nm using UV-visible spectroscopy. The formula for calculating antioxidant activity was as follows [8]:

$$\text{DPPH scavenging (\%)} = (A_c - A_s) \times 100$$

where,  $A_c$  was absorbance of the uncoated apples (control) and  $A_s$  was absorbance of the coated apples.

### 2.6.6. In-vitro release analysis in phosphate buffer saline

To study release of resveratrol in apples, coated and uncoated apples were analyzed. Uncoated apples were used as controls. For the coated apples, 5 mg of the extract were incubated in 1.5 ml of phosphate buffer saline (PBS) (pH 7.2) and transferred into dialysis bag. Dialysis bag was immersed into 50 ml of release media and incubated at 37 °C with gentle agitation. Using 1-h time intervals, 1 ml of the release media was collected and replaced with fresh release media. Then, absorbance was measured at 305 nm using UV-visible spectroscopy [11].

### 2.6.7. Encapsulation efficiency of the loaded resveratrol

Loaded resveratrol in  $\beta$ -lg nanofibrils was calculated using UV visible spectroscopy. Briefly, 2mg of the nanofibrils were added into 1 ml of double DW and centrifuged at 10483 $\times$ g for 30 min to remove unloaded resveratrol. Pellet was dissolved in 80% ethanol and analyzed at 305 nm using UV-visible spectroscopy. Encapsulation efficiency of the loaded resveratrol was calculated using Eq. 3:

$$\text{Encapsulation efficiency(\%)} = \frac{\text{Amount of resveratrol in pellet (R}_P\text{)}}{\text{Total amount of the untrapped resveratrol (R}_F\text{)}} \times 100 \quad \text{Eq.3}$$

## 3. Results and Discussion

### 3.1 Preparation of nanofibrils and nano composite fibrils

At optimal self-assembly conditions, formation of the well-defined semi-flexible  $\beta$ -lg nanofibrils was carried out, as shown in the schematic Figure 1. By decreasing pH and increasing temperature, the fibrillation process occurred; in which, small peptide fragments and spontaneous fibrils were formed via hydrolysis of protein [14]. To prepare resveratrol-loaded nanofibrils, resveratrol was dissolved in water, carefully mixed with  $\beta$ -lg solutions and incubated at 80 °C for 10 h. Higher concentrations of the resveratrol were formed as precipitates or aggregates while mixing with  $\beta$ -lg solutions due to the poor water solubility.

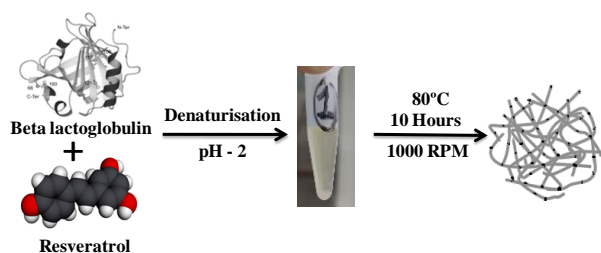


**Figure 1.** Schematic representation of formation of nanofibril composites using self-assembly method.

A concentration of 0.02 mg in 1 ml was the ideal ratio to prepare resveratrol-loaded nano composite fibrils. The underlying mechanism between the resveratrol and  $\beta$ -lg protein is unknown; however, formation of the nano composite fibrils is majorly driven by the interactions, including hydrogen bonds, peptide linkages and hydrophilic/hydrophobic affinities; as shown for the formation of individual nanofibrils.

### 3.2 Characterization of $\beta$ -lg nanofibrils

Morphology of the prepared  $\beta$ -lg nanofibrils was characterized using AFM and SEM. Figure 2a, shows formation of the homogeneous nanofibrils with well-defined nanostructures. Diameter of the nanofibrils varied from 0.5 nm to more than 20 nm ( $n = 251$ ); as shown in height and length histograms (Figure 2b, c). However, the most predominated fibril populations included 4-6 nm nanofibrils, whereas nanofibrils greater than 10 nm were attributed to the bundling effects during the fibril formation. Ikeda and Morris were the first to use AFM in contact mode to capture the formed fibrils. Fine-stranded structures (e.g. short flexible fibrils) of 4-nm diameter were observed when aggregated at pH 2 and incubated at 80 °C [15]. Arnaudov and his colleagues used low pH and ionic conditions and reported long-straight fibrils with height modulation in their length of 25 nm [16]. Short flexible structures were seen when the protein was assembled in water-alcohol mixtures at pH 2 and neutral pH [17]. Adamcik et al. in 2016 were able to produce detailed structural hierarchic assembly of nanofibrils from 2, 4, 6, 8 and 10 nm [18]. In contrast, the current study produced mostly 4-6 nm fibrils. This could be due to the lack of high resolution AFM imaging and slight changes in the experimental protocols. Nevertheless, the present AFM images of  $\beta$ -lg nanofibrils from this study were similar to those of other studies. Lengths of the nanofibrils varied from few to several micrometers ( $n=81$ ) (Figure 2c). Furthermore, SEM images revealed formation of well-defined uniform nanofibrils (Figure 2d).

### 3.3 Characterization of resveratrol-loaded $\beta$ -lg nanofibrils

Morphology of resveratrol loaded  $\beta$ -lg nanofibrils was characterized using AFM and SEM; similar to  $\beta$ -lg nanofibrils.

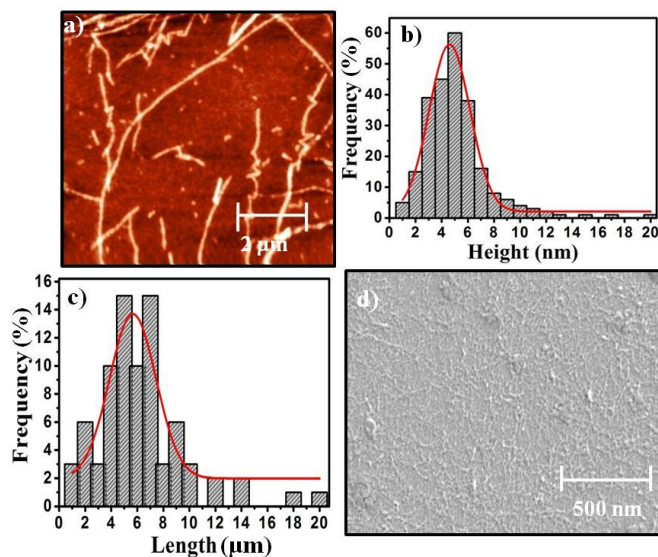


**Figure 2.** a) AFM height image, b) Height histogram, c) Length histogram and d) SEM image of  $\beta$ -lg nanofibrils.

Figure 3 shows the morphology of nanofibrils with changes compared to those in Figure 2 due to the attachment of the resveratrol into the  $\beta$ -lg nanofibrils. For  $\beta$ -lg nanofibrils, surface of the nanofibrils were smooth, whereas surface of the resveratrol-loaded  $\beta$ -lg nanofibrils was rough (Figure 3a). Heights (representative of the fibril diameter) of the nanofibrils varied 6-10 nm (fibrils larger than 10nm were due to the bundling) ( $n=215$ ) and lengths varied from 1 to several micrometers ( $n=73$ ) (Figure 3b, c. Data from AFM were verified using SEM images (Figure 3d). Although resveratrol-loaded nanofibrils formed more aggregates, compared to  $\beta$ -lg nanofibrils. Based on the AFM and SEM images, it might not be possible to conclude whether resveratrol was attached to the nanofibrils due to the lack of high resolution imaging of AFM or periodicity of the nanofibrils; therefore, other complementary techniques were used.

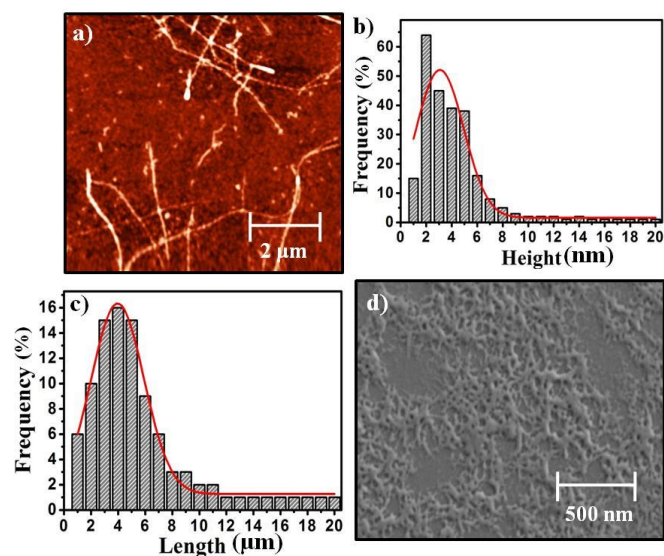


**Figure 3.** a) AFM height image, b) Height histogram, c) Length histogram and d) SEM image of Resveratrol loaded  $\beta$ -lg nanofibrils.

### 3.4 Fourier-transform infrared spectroscopy

Generally, FT-IR spectra were used to assess the functional group of the prepared nanofibrils. The O-H stretching at  $1317\text{ cm}^{-1}$  was identified in the FT-IR spectra of resveratrol due to the presence of alcoholic group and C-C olefinic stretching was identified at  $1639\text{ cm}^{-1}$ . The  $\text{-C=C-}$  stretching at  $690\text{ cm}^{-1}$  was reported in the Trans form of the resveratrol. Incorporation of resveratrol into  $\beta$ -lg matrix resulted in decreased ending and stretching of the bonds; hence, most representative peaks of the resveratrol disappeared in its nanoencapsulated form. Development of the hydrogen bonds between  $\beta$ -lg and active molecules resulted new bond formation or shift of the peaks at  $3200\text{--}3400\text{ cm}^{-1}$ . The peak of  $1317\text{ cm}^{-1}$  indicated hydrogen bonds for native resveratrol, whereas shift in the peak of  $1192\text{ cm}^{-1}$  indicated formation of hydrogen bonds between  $\beta$ -lg and resveratrol; showed in SI 1.

### 3.5 In-vitro release from phosphate buffer saline

To assess attachment and sustainable release of the resveratrol-loaded  $\beta$ -lg nanofibrils, *in-vitro* release assessment was carried out using dialysis bag method. The resveratrol release against time was shown in Figure 4a.

Sustainable release of the resveratrol was seen from  $\beta$ -lg nanofibrils with respect to time upto 7 h of the study. Several researchers have studied various kinetics models to understand release of the loaded molecules from the attached nanofibrils [19-21]. Based on the kinetics models and previous studies, the sustainable release of resveratrol was due to the relaxation of  $\beta$ -lg matrixes, diffusion and surrounding media. To verify *in-vitro* assessment results, resveratrol-loaded  $\beta$ -lg was coated on apple slices using dipping method. Figure 4b, c shows that the uncoated apples include more enzymatic browning after few minutes, whereas the coated apples with nanofibril solution include less enzymatic browning due to the controlled release of loaded resveratrol.

### 3.6. Analysis of nanofibril-coated apples

#### 3.6.1. Weight loss, total acidity and color measurements

First, weight loss for the coated and uncoated sliced apples was negligible. A gradual weight loss was observed for the coated apples, whereas increased weight loss was seen for the uncoated apples (Figure 5a). Weight loss in uncoated apples was due to the biochemical activities such as transpiration and respiration, whereas coated apples were protected by the nanofibril networks; hence, weight loss was

minimized [22]. Acidity of the apples was controlled by the effects of coating through retarding the respiration rate. Acidity of the coated apples was constant at  $2.23\% \pm 0.02$ , whereas asymmetrical variations were reported for the uncoated apples ( $2.00\% \pm 0.02$  to  $2.22\% \pm 0.02$ ) (Figure 5b). The metabolic process in respiration break downs organic materials using atmospheric conditions. Moreover, coating prevents the break down by interfering with atmospheric parameters such as gases and energies [23]. Table ST1 shows the assessed values of WI, C and  $\Delta E$ . As expected, WI values decreased at acidic conditions, whereas WI values increased in resveratrol and resveratrol-loaded  $\beta$ -lg nanofibrils after Hour 5. Therefore, total color difference for the resveratrol-loaded  $\beta$ -lg nanofibrils increased  $\sim 45\%$  due to the sustainable release of the resveratrol, which can be used to increase the shelf-life and freshness of the fruits.

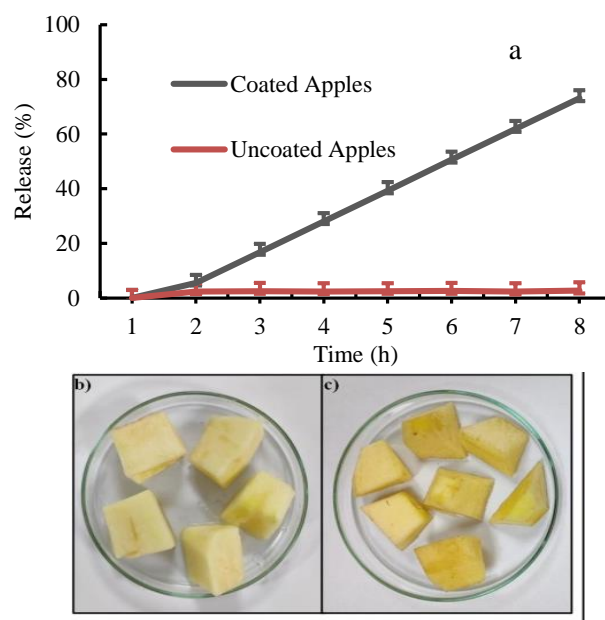


**Figure 4.a** *In-vitro* release study of coated and uncoated resveratrol loaded nanofibrils of sliced apples, b) Coated and c) Uncoated sliced apples.

#### 3.6.2. Encapsulation efficiency

From the Table 1, the highest encapsulation efficiency was achieved for 1% resveratrol-loaded  $\beta$ -lg nanofibrils. Bhushani et al. reported that as zein content increased, the encapsulation efficiency decreased; as shown by the current data [24].

**Table 1.** Encapsulation efficiency of  $\beta$ -lg nanofibrils and resveratrol loaded  $\beta$ -lg nanofibrils

Formulation	$\beta$ -lg Concentration (%W W <sup>-1</sup> )	Resveratrol concentration (%W W <sup>-1</sup> )	Encapsulation efficiency (%)
$\beta$ -lg nanofibrils	2	0	0
Resveratrol loaded $\beta$ -lg nanofibrils	2	1	$61 \pm 0.74$
	2	1.5	$47 \pm 0.51$
	2	2	$42 \pm 0.96$

### 3.6.3. Total phenolic content assay

Total phenolic content (TPC) of the coated and uncoated samples was analyzed using gallic acid as standard. The TPC was 2.56 mg GAEg<sup>-1</sup> in uncoated apples and 4.87 mg GAEg<sup>-1</sup> in coated apples (Figure 5c). Decreased TPC in uncoated apples was because of the elimination of vitamin C [25], whereas elimination of vitamin C in coated apples was controlled by the resveratrol-loaded nanofibril network structures.

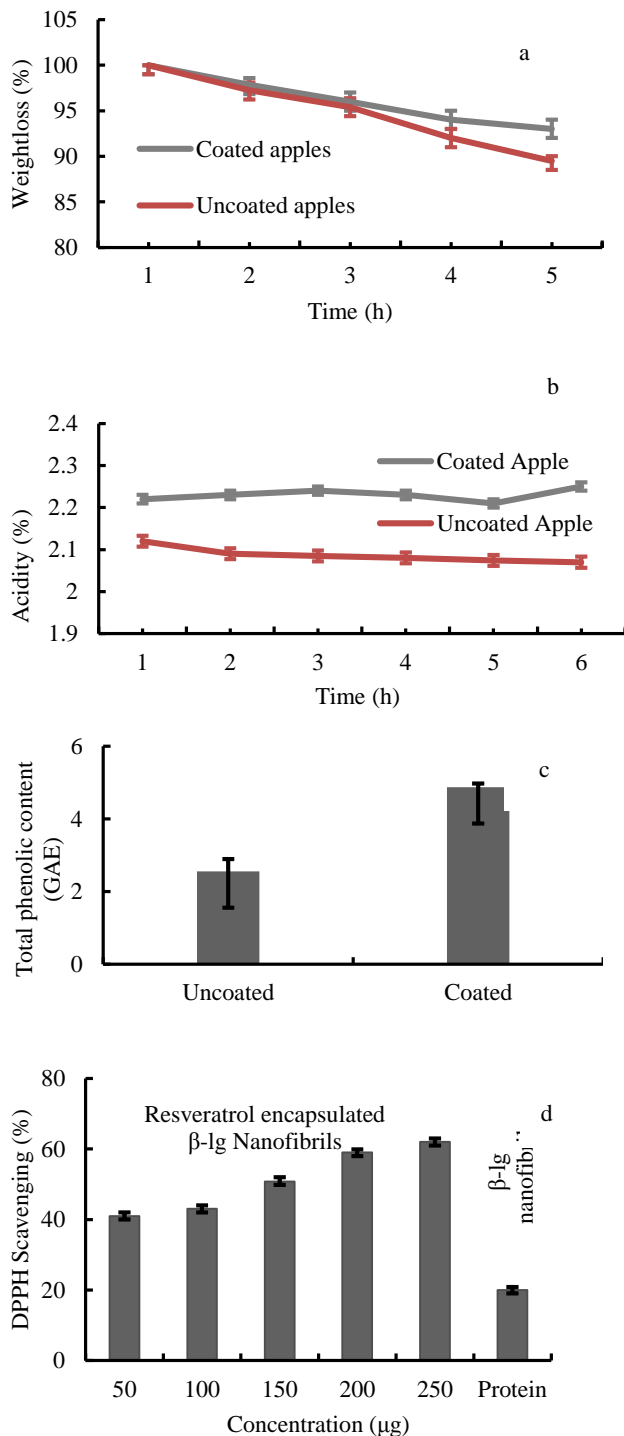


**Figure 5.** a) Weight loss measurements, b) Titratable acidity, c) Total phenolic content and d) Anti-oxidant activity of sliced apples.

### 3.6.4. Antioxidant activity

Antioxidant activity of the loaded resveratrol and controlled nanofibrils were assessed using DPPH scavenging capacity method. Controlled nanofibrils and loaded resveratrol showed DPPH activity. Controlled  $\beta$ -lg showed 20% of antioxidant activity due to the presence of amino acids. Antioxidant activities of the resveratrol-loaded nanofibril varied 40-60% (Figure 5d). By increasing concentration of the resveratrol-loaded nanofibrils from 50 to 250  $\mu$ l, antioxidation activities gradually increased due to the scavenging activity of the component. This helped delay rancidity and preserve nutritional characteristics and quality of the food product.

## 4. Conclusion

Resveratrol-loaded  $\beta$ -lg nanofibrils were successfully prepared using simple self-assembly method. The AFM and SEM were used to study morphology of the composite nanofibrils, which showed that the diameter varied 6-10 nm. Efficiency of the resveratrol-loaded nanofibrils was studied using various assays, including *in-vitro* release, weight loss, total acidity, TPC and antioxidant activity. Results showed the sustainable release of resveratrol from the nanofibrils, the bioavailability and significant decreases in enzymatic browning of the sliced apples for upto 5 h. Therefore, results have verified that the self-assembly method includes high potentials to prepare well-defined resveratrol-loaded nanofibrils, which can be used as an edible coating of foods and nutraceutical-based foods.

## 5. Acknowledgements

This study was financially supported by Department of Science and Technology (DST) (grant no INT/RUS-/RFBR/367) and RFBR (grant no 19-57-45024) under international bilateral cooperation between the governments of India and Russia.

## 6. Conflict of Interest

The authors report no conflicts of interest.

## References

- Teo WE, Ramakrishna S. A review on electrospinning design and nanofibre assemblies. *Nanotechnol*. 2006;17(14): 89-106. doi:10.1088/0957-4484/17/14/R01
- Hong J, Yeo M, Yang GH, Kim G. Cell-electrospinning and its application for tissue engineering. *Int J Mol Sci*. 2019;20(24): 6208, 1-14. doi:10.3390/ijms20246208
- Suvannasara P, Praphairaksit N, Muangsin N. Self-assembly of mucoadhesive nanofibers. *RSC Adv*. 2014;4(102):58664-58673. doi:10.1039/c4ra09329a
- Drosou C, Krokida M, Biliaderis CG. Composite pullulan-whey protein nanofibers made by electro-spinning: Impact of

- process parameters on fiber morphology and physical properties. *Food Hydrocoll.* 2018;77:726-735. doi:10.1016/j.foodhyd.2017.11.014
5. Eissa AS, Khan SA. Acid-induced gelation of enzymatically modified, preheated whey proteins. *J Agric Food Chem.* 2005;53(12):5010-5017. doi:10.1021/jf047957w
  6. Jung JM, Savin G, Pouzot M, Schmitt C, Mezzenga R. Structure of heat-induced  $\beta$ -lactoglobulin aggregates and their complexes with sodium-dodecyl sulfate. *Biomacromolecules* 2008;9(9):2477-2486. doi:10.1021/bm800502j
  7. Dave AC, Loveday SM, Anema SG, Loo TS, Norris GE, Jameson GB, Harjinder Singh.  $\beta$ -lactoglobulin self-assembly: Structural changes in early stages and disulfide bonding in fibrils. *J Agric Food Chem.* 2013;61(32):7817-7828. doi:10.1021/jf401084f
  8. Jayan H, Maria Leena M, Sivakama Sundari SK, Moses JA, Anandharamakrishnan C. Improvement of bioavailability for resveratrol through encapsulation in zein using electrospraying technique. *J Funct Foods.* 2019;57:417-424. doi:10.1016/j.jff.2019.04.007
  9. Lin YC, Hu SCS, Huang PH, Lin TC, Yen FL. Electrospun resveratrol-loaded polyvinylpyrrolidone/cyclodextrin nanofibers and their biomedical applications. *Pharm.* 2020;12(6):1-16.
  10. Busolo MA, Lagaron JM. Antioxidant polyethylene films based on a resveratrol containing clay of Interest in food packaging applications. *Food Packag Shelf Life* 2015;6:30-41. doi:10.1016/j.fpsl.2015.08.004
  11. Maria Leena M, Yoha KS, Moses JA, Anandharamakrishnan C. Edible coating with resveratrol loaded electrospun zein nanofibers with enhanced bioaccessibility. *Food Biosci.* 2020; 36 (100669): 1-10. doi:10.1016/j.fbio.2020.100669
  12. Sanna V, Roggio AM, Pala N, Marceddu S, Lubinu G, Mariani A, Sechi M. Effect of chitosan concentration on PLGA microcapsules for controlled release and stability of resveratrol. *Int J Biol Macromol.* 2015;72:531-536. doi:10.1016/j.ijbiomac.2014.08.053
  13. Garner D, Crisosto CH, Wiley P, Crisosto GM. Measurement of pH and titratable acidity. *Qual Eval Methodol.* 2003.
  14. Kamada A, Mittal N, Soderberg LD, Ingverud T, Ohm W, Roth S V. Flow-assisted assembly of nanostructured protein microfibers. 2017;114(6):1232-1237. doi:10.1073/pnas.1617260114
  15. Ikeda S, Morris VJ. Fine-stranded and particulate aggregates of heat-denatured whey proteins visualized by atomic force microscopy. *Biomacromolecules* 2002;3(2):382-389. doi:10.1021/bm0156429
  16. Arnaudov LN, De Vries R. Thermally induced fibrillar aggregation of hen egg white lysozyme. *Biophys J.* 2005;88(1):515-526. doi:10.1529/biophysj.104.048819
  17. Gosal WS, Clark AH, Pudney PDA, Ross-Murphy SB. Novel amyloid fibrillar networks derived from a globular protein:  $\beta$ -lactoglobulin. *Langmuir* 2002;18(19):7174-7181. doi:10.1021/la025531a
  18. Adamcik J, Dmitry V, Guillaume W, Sergey KS, Giovanni D. Observation of single-stranded DNA on mica and highly oriented pyrolytic graphite by atomic force microscopy. *FEBS letters* 2006;580:5617-5675.
  19. Antoniraj G M, Leena MM, Moses JA, Anandharamakrishnan C. Cross-linked chitosan microparticles preparation by modified three fluid nozzle spray drying approach. *Int J Biol Macromol.* 2020;147:1268-1277. doi:10.1016/j.ijbiomac.2019.09.254
  20. Siepmann J, Peppas NA. Modeling of drug release from delivery systems based on hydroxypropyl methylcellulose (HPMC). *Adv Drug Deliv Rev.* 2001;48(2-3):139-157. doi:10.1016/S0169-409X(01)00112-0
  21. Rezaei A, Nasirpour A, Tavanai H, Fathi M. A study on the release kinetics and mechanisms of vanillin incorporated in almond gum/polyvinyl alcohol composite nanofibers in different aqueous food simulants and simulated saliva. *Flavour Fragr J.* 2016;31(6):442-447. doi:10.1002/ffj.3335
  22. Abu RP, O'Connor K, Seeram R. Current progress on bio-based polymers and their future trends. *Prog Biomater.* 2013;2(1):8. doi:10.1186/2194-0517-2-8
  23. Al-Juhaimi F, Ghafoor K, Babiker EE. Effect of gum arabic edible coating on weight loss, firmness and sensory characteristics of cucumber (*cucumis sativus* L.) fruit during storage. *Pakistan J Bot.* 2012; 44(4): 1439-1444.
  24. Anu Bhushani J, Anandaramakrishnan C. Electrospinning and electrospraying techniques: Potential food based applications. *Trends Food Sci Technol.* 2014; 38(1):21-33. doi:10.1016/j.tifs.2014.03.004.
  25. Lopez-Velez M, Martinez-Martinez F, Valle-Ribes C Del. The Study of Phenolic compounds as natural antioxidants in Wine. *Crit Rev Food Sci Nutr.* 2003;43(2):233-244. doi:10.1080/10408690390826509



## نانوفیبریل های بتا-لاکتوگلوبولین بارگذاری شده با رسوراترول برای جلوگیری از قهوه ای شدن آنزیمی برش های سیب

پراویتا سنتیل کومار<sup>۱</sup>، ولادیمیر شاوروف<sup>۲</sup>، پتر لگا<sup>۳</sup>، رامش سوبرمانی<sup>\*۱</sup>

<sup>۱</sup> گروه مدیریت و تکنولوژی فرایند مواد غذایی، کالج زنان PSGR کریشنامال، کویمباتور، تامیلنادر، هند.

<sup>۲</sup> انستیتو مهندسی رادیو و الکترونیک کولتلیکوف، آکادمی علوم روسیه، مسکو، ۱۲۵۰۰۹، روسیه.

### تاریخچه مقاله

دریافت ۲ آگوست ۲۰۲۱

داوری ۲۶ آگوست ۲۰۲۱

پذیرش ۲۵ اکتبر ۲۰۲۱

### واژگان کلیدی

- بتا-لاکتوگلوبولین
- نانوفیبریل های
- رسوراترول
- سیب
- خودگردایش

### \*نویسنده مسئول

رامش سوبرمانی

گروه مدیریت و تکنولوژی فرایند مواد غذایی، کالج زنان PSGR کریشنامال، کویمباتور، تامیلنادر، هند.

تلفن: ۹۱ ۶۳۸۰۲۳۲۴۰۲ +

پست الکترونیک:

ramesh.subramani@psgrkcw.ac.in

### چکیده

**سابقه و هدف:** رسوراترول پلی فنولی با فواید غذا-دارویی بر سلامتی است که برای اثرات ضد سرطانی، آنتی اکسیدانی، ضدالتهابی و محافظتی قلب مورد استفاده قرار می گیرد. با این حال، رسوراترول فاقد حلالیت و زیست‌فراهمی است و تحت تاثیر نور فرابنفش قرار می گیرد که کاربردش در صنایع غذایی را کاهش می دهد. با بارگذاری رسوراترول با ترکیبات زیستی مناسب، امکان غلبه بر این مشکلات وجود دارد. بتا-لاکتوگلوبولین قادر به تشکیل نانوفیبریل های کاملاً مشخص با کاربردهای گوناگون است. هدف این مطالعه کاربرد فیبریل های بتا-ایمونوگلوبولین در مقیاس نانو به منظور افزایش زیست‌فراهمی رسوراترول و حفظ تازه گی و جلوگیری از قهوه ای شدن آنزیمی برش های سیب بود.

**مواد و روش ها:** نانوفیبریل های چندسازه<sup>۱</sup> جدید با بارگذاری رسوراترول روی نانوفیبریل های بتا-لاکتوگلوبولین به روش خودگردایش<sup>۲</sup> ساده تهیه شدند. علاوه بر این، به منظور تایید رهایش پایدار ترکیبات زیست‌شیمیایی<sup>۳</sup> و زیست-فراهمی<sup>۴</sup> مطالعات توسط میکروسکوپ نیروی اتمی<sup>۵</sup> میکروسکوپ الکترونی روبشی<sup>۶</sup>، بررسی برون تنی<sup>۷</sup> رهایش، افت وزن، اسیدیته تام، میزان کل ترکیبات فنولی و فعالیت آنتی اکسیدانی انجام شد.

**یافته ها و نتیجه گیری:** تصاویر تهیه شده توسط میکروسکوپ نیروی اتمی و میکروسکوپ الکترونی روبشی تشکیل نانوفیبریل های چندسازه را با بزرگنمایی متوسط ۱۰۰۰ بخوبی نشان داد. بررسی برون تنی رهایش نشان داد که به علت تداخل های احتمالی پیوندهیدروژن و سایر پیوندهای غیر کووالانسی، رسوراترول به طور موفقیت آمیزی روی نانوفیبریل ها بارگذاری شد. بالاترین کارایی ریزپوشانی<sup>۸</sup> ۶۱/۱٪، با کمترین غلظت رسوراترول (۱۰ میلی گرم در ۱ میلی لیتر) به دست آمد در حالی که، برای بالاترین غلظت رسوراترول (۲۰ میلی گرم در ۱ میلی لیتر)، کارایی ریزپوشانی ۴۸/۳٪ بود. بررسی افت وزن، اسیدیته کل، رنگ، میزان کل ترکیبات فنولی و فعالیت آنتی اکسیدانی نشان داد به علت بهبود زیست‌فراهمی رسوراترول، عمر انباری<sup>۹</sup> و پیشگیری از قهوه ای شدن آنزیمی تقریباً به میزان ۵۰٪ افزایش می یابد. مطالعه حاضر به طور موفقیت آمیزی توانایی آنتی اکسیدانی رسوراترول در برش های سیب و کمک به حفاظت بهتر در برابر کهنگی<sup>۱۰</sup> را نشان داد. این فرمول می تواند به عنوان لایه محافظ روی فرآورده های غذایی با ارزش مانند میوه های مستعد به شرایط فساد مورد استفاده قرار گیرد.

**تعارض منافع:** نویسندگان اعلام می کنند که هیچ نوع تعارض منافی مرتبط با انتشار این مقاله ندارند.

<sup>1</sup> Composite

<sup>2</sup> Self-assembly

<sup>3</sup> Biochemical

<sup>4</sup> Bioavailability

<sup>5</sup> Atomic force microscopy

<sup>6</sup> Scanning electron microscopy

<sup>7</sup> in-vitro

<sup>8</sup> Encapsulation efficiency

<sup>9</sup> Shelf-life

<sup>10</sup> Ageing

